At-Scale Sparse Deep Neural Network Inference With Efficient GPU Implementation

Mert Hidayetoğlu, Carl Pearson, Vikram Sharma Mailthody, Eiman Ebrahimi[‡],
Jinjun Xiong[§], Rakesh Nagi, and Wen-mei Hwu
University of Illinois at Urbana-Champaign, [‡]NVIDIA, [§]IBM Research
{hidayet2, pearson, vsm2}@illinois.edu, eebrahimi@nvidia.com, jinjun@us.ibm.com, {nagi,w-hwu}@illinois.edu

Abstract—This paper presents GPU performance optimization and scaling results for inference models of the Sparse Deep Neural Network Challenge 2020. Demands for network quality have increased rapidly, pushing the size and thus the memory requirements of many neural networks beyond the capacity of available accelerators. Sparse deep neural networks (SpDNN) have shown promise for reining in the memory footprint of large neural networks. However, there is room for improvement in implementing SpDNN operations on GPUs. This work presents optimized sparse matrix multiplication kernels fused with the ReLU function. The optimized kernels reuse input feature maps from the shared memory and sparse weights from registers. For multi-GPU parallelism, our SpDNN implementation duplicates weights and statically partition the feature maps across GPUs. Results for the challenge benchmarks show that the proposed kernel design and multi-GPU parallelization achieve up to 180 TeraEdges per second inference throughput. These results are up to 4.3× faster for a single GPU and an order of magnitude faster at full scale than those of the champion of the 2019 Sparse Deep Neural Network Graph Challenge for the same generation of NVIDIA V100 GPUs. Using the same implementation[1], we also show single-GPU throughput on NVIDIA A100 is 2.37× faster than V100.

I. INTRODUCTION

Deep learning (DL) has seen great progress over the last decade and demonstrated substantial accuracy improvement over a range of machine learning tasks such as image classification [1], object recognition [2], language modeling [3], [4], and language translation [5]. Scaling up DL models along with increased amount of training data have proven to be an effective approach to improve the model accuracy [3], [4], [6]. The progress of DL applications involves not only the algorithmic improvements, but also the unprecedented computational throughput provided by GPUs.

On several machine learning tasks, the size of state-of-the-art deep neural networks (DNN) has grown beyond the memory limits of available accelerators [3], [6]. To address this, the DL community has taken an algorithmic approach of sparsifying the DNN using techniques such as pruning [7]–[9]. These optimization convert a dense DNN into a sparse DNN.

Sparse DNNs present unique scalablity challenges. Realizing this, in 2019 MIT/IEEE/Amazon proposed the Sparse DNN Challenge as an extension to the Graph Challenge [10]–[14]. The Sparse DNN Challenge is created by leveraging the

collective knowledge of machine learning, high-performance computing and graph analytics communities on emerging AI systems. The objective of the Sparse DNN Challenge is to build scalable algorithms and systems for sparse AI analytics.

The Sparse DNN Challenge provides model structure, trained model weights, and inputs as a foundation for comparison of inference performance. Several models with varying number of layers (120 to 1920 layers) and neuron connections (4 Million to 4 Billion) are posted in the challenge. Such a large variation allows system and algorithm designers to evaluate efficient, scalable implementations against a variety of network types.

In this work, we propose efficient sparse algorithms and demonstrate performant kernel implementations for sparse DNN inference on GPUs. GPUs have become a de-facto accelerator for DNN computation. However, traditionally GPUs are designed for *dense* DNN operations and their performance is considerably reduced for *sparse* DNN computations. Using a baseline sparse DNN implementation, we identify the causes of performance bottlenecks. In our baseline implementation, we store the weights as sparse matrices in the compressed sparse row (CSR) storage format while the inputs are represented as dense matrices in the column-major data layout in memory. We observe that irregular memory accesses to the input matrix and redundant accesses to the weight matrices are the primary causes for inefficiency in the naive sparse DNN implementation.

To address this, we propose a few optimizations, namely, register tiling, shared-memory tiling, and compact index representation to create optimized kernel implementation fused with ReLU activation for sparse DNN inference. In the optimized fused kernel, the weights are stored in sliced ELLPACK format for efficient memory access while the inputs are retained in the column-major layout in memory. Together these optimizations minimize the total number of irregular memory access and redundant access to the global memory, thus providing significant performance improvements. Although variants of these optimizations have been applied in sparse matrix mutiplication (SpMM) kernels [15] [16], in this work we tune them for sparse DNN computation.

Our evaluation shows, compared to the baseline fused kernel implementation, the optimized fused kernel provides up to 11.84× speedup. Overall, the proposed optimizations achieve up to 14.30 TeraEdges, i.e., 10^{12} edges, per second perfor-

---

mance on a single V100 GPU. Compared with prior champions, our single GPU implementation on the same generation of NVIDIA Volta V100 GPU is up to $4.3\times$ faster. Compared to an implementation based off of NVIDIA's cuSPARSE, our proposed kernels can provide $200\times$ speedup. In addition, we evaluate the performance of our optimized fused kernel on the latest generation NVIDIA Ampere A100 GPU, and show that out-of-the-box execution of our optimized kernel achieves up to 20.99 TeraEdges per second ($2.37\times$ faster than V100 GPU).

To measure the algorithm scalablity, we perform strong scaling using batch parallelism and scale up to 768 V100 GPUs on department of energy's Summit supercomputer at Oak Ridge National Laboratory [17]. On a single node, when the number of V100 GPUs are increased from one to six, optimized fused kernel achieves up to $5.37\times$ speedup, and thus providing a scaling efficiency of 89.5%. Our evaluation shows that, our proposed implementation can provide up to $51.8\times$ speed up when the number of GPUs is increased to 768 (or 128 nodes with 6 GPUs in each node) compared to the single V100 GPU implementation. Compared to 2019 Sparse DNN Champions, our scale-out implementation is 3.25–$19.13\times$ faster, providing up to 180 TeraEdges per second.

Overall, we make the following main contributions:
1) We present novel fused SpMM kernel design that is optimized for providing data reuse during DNN inference.
2) We perform extensive at-scale benchmarking on up to 768 V100 GPUs as well as the new A100 GPUs for the Sparse Deep Neural Network Challenge dataset.

II. BACKGROUND & MOTIVATION

In this section, we provide a brief overview of the Sparse DNN Challenge and discuss the limitations in naive sparse DNN inference implementation.

A. Overview of Sparse DNN Challenge

The Sparse DNN Challenge specifies a collection of large sparse DNNs models [10], [11] that are representative of the latest trends in addressing challenging machine learning tasks. The challenge provides model structure (number of layers and size of layer), and model weights for computing sparse DNN inference on a given input dataset.

1) Formulation of Sparse Layer: For a sparse DNN with L layers, each sparse layer computation can be formulated as

$$Y_{l+1} = \text{ReLU}(W_l \times Y_l + B) \tag{1}$$

where l is the layer number, Y_l and Y_{l+1} are $N \times M$ matrices of M input and output features of length N, respectively, stored in column-major format, W_l is an $N \times N$ matrix of activation weights, B_l is an $N \times M$ bias matrix for each output, and ReLU is the activation function. Here, ReLU activation function promotes sparsity and is defined as $\text{ReLU}(x) = \max\{0, \min\{x, 32\}\}$. The weight matrix represents a general pattern of neuron connections: for a fully-connected layer, W_l would be entirely non-zero, for a convolution layer, W_l would be banded, and for a general sparse layer, W_l is a general sparse matrix.

2) Steps Involved in Sparse DNN Challenge: Algorithm 1 describes the high-level steps involved in computing sparse DNN inference in the Sparse DNN Challenge [10], [18]. The challenge provides datasets comprising of input data for the neural network, weights for each layer in the network, bias values for each layer and finaly the ground truth to validate if the results are correct while computing inference.

Algorithm 1 Outline of Sparse DNN Challenge Algorithm
1: Read input Y_0 and model weights (W_0, W_1 ... W_{L-1}) from binary files
2: Initialize bias vector B with a constant
3: Evaluate Equation (1) for all the layers, starting from $l = 0$ and until $l = L - 1$
4: Use Y_{L-1} to determine categories and compare with the ground truth.
5: Measure and report performance

The input to the neural network is an interpolated sparse version derived from the MNIST dataset and consists of 60,000 images stored in TSV format. Each of the MNIST 28×28 pixel images are resized to 32×32 (1024 neurons), 64×64 (4096 neurons), 128×128 (16384 neurons) and 256×256 (65536 neurons) pixels. All resized images are thresholded to ensure values reside between 0 to 1. Then, they are linearized and stacked together to obtain 60k1K, 60k4K, 60k16K, and 60k64K input feature matrices. This allows to store each image in a single row in the TSV while each column representing a non-zero pixel location with a value of 1. The challenge also provides three different sparse DNN models comprising of 120, 480, and 1920 layers. Thus effectively creates a total of 12 DNNs ({1024, 4096, 16384, 65536} neurons $\times$ {120, 480, 1920} layers), publicly available [19].

Since such large sparse DNN networks are not publicly available, the challenge generates the weight matrix using RadiX-Net synthetic sparse DNN generator [8]. The synthetic generator is capable of creating pre-determined DNNs with 32 connections per neuron and ensuring there exists an equal number of paths between inputs and intermediate layers. All neurons have weights and biases set to 1/16. However, our kernel design and implementation could work on real-life data with any arbitrary bias values and any sparse layer with an arbitrary sparsity pattern.

B. The Baseline GPU Implementation

We present a baseline implementation of sparse DNN using GPUs and discuss the bottlenecks to motivate our optimizations. The baseline implementation consists a sparse$\times$dense SpMM kernel fused with ReLU function for GPU execution. In this implementation, shown in Listing 1, each thread produces a single output element in Y_{l+1}, and gathers data from the corresponding column of Y_l. Each thread reads a row of `windex` (column indices of non-zero weight elements in the CSR format) and `wvalue` (the value of the non-zero weight elements) from sparse W_l matrix stored in CSR format, as depicted in Figure 1. Note that `windex` and `wvalue` have

the same layout and access patterns so we omitted `wvalue` from Figure 1. Also, each `wdispl` element gives the starting location of its corresponding row of non-zero elements in the CSR format. That is, all `windex` elements in Figure 1 are stored in a linear array with the starting point of each row of non-zero elements delineated by the `wdispl` elements.

Listing 1: Baseline Implementation

```
1   __device__ float __ReLU(float x){
2     return x<0.0?0.0:x>32.0?32.0:x;
3   };
4   __global__ void fused_ReLU(float *yout, float *yin, int neuron,
5    int *wdispl, int *windex, float *wvalue, float *bias, int *active,
6    int *category){
7     int xoff = blockIdx.x*blockDim.x+threadIdx.x;
8     int yoff = category[blockIdx.y]*neuron;
9     float acc = 0;
10    for(int n = wdispl[xoff]; n < wdispl[xoff+1]; n++)
11      acc += yin[yoff+windex[n]]*wvalue[n];
12    acc = __ReLU(acc+bias[xoff]);
13    if(acc > 0){
14      yout[blockIdx.y*neuron+xoff] = acc;
15      atomicAdd(active+blockIdx.y,1);
16    }
17  }
18
19  //INFERENCE LOOP AT HOST CPU
20  for(int l = 0; l < layer; l++){
21    dim3 grid(neuron/blocksize,mybatch);
22    dim3 block(blocksize);
23    cudaMemset(active_d,0,sizeof(int)*mybatch);
24    fused_ReLU<<<grid,block>>>(nextfeat_d,currfeat_d,neuron,
25     wdispl_d[l],wind_d[l],wval_d[l],bias_d,active_d,categories_d);
26    cudaMemcpy(active,active_d,sizeof(int)*mybatch,D2H);
27    int feature = 0;
28    for(int k = 0; k < mybatch; k++){
29      if(active[k]){
30        globalcategories[feature] = globalcategories[k];
31        categories[feature] = k;
32        feature++;
33      }
34    }
35    cudaMemcpy(categories_d,categories,sizeof(int)*feature,H2D);
36    mybatch = feature;
37    FEATPREC *tempfeat_d = currfeat_d;
38    currfeat_d = nextfeat_d;
39    nextfeat_d = tempfeat_d;
40  }
```

For simplicity in the figure, we assume a toy example where each block consists of four threads and the warp size is two. As a result, the GPU kernel deploys N/B thread blocks for each feature, where N is the number of output feature elements (pixels), and B is the block size. Here, each block accesses a portion of $\boldsymbol{W}_l$. As each thread accesses the input, it performs a fused multiply-and-add (FMA) operation with the corresponding activation weight, accumulating the result in its register `acc`. Finally, each thread adds the bias and activate (or deactivate) the output, and writes the output to global memory.

While the baseline implementation exhibits a high degree of thread-level parallelism for large output features, it is inefficient for several reasons. First, the global memory accesses to the input matrix are not only uncoalesced, but also irregular: Figure 1 highlights the memory accesses of the first thread of the first block. An iregular subset of the $\boldsymbol{Y}_l$ elements are read by each thread. Second, threads that generate equivalent elements in different output maps redundantly reads the same row of the $\boldsymbol{W}_l$ matrix. As a result the weight matrix is read M times. This results in wasting memory bandwidth that could have been used for the needed computation. Third, the load imbalance among threads caused by different number of non-zero elements in adjacent rows of $\boldsymbol{W}_l$ yields thread divergence within warps. We address these limitation in the next section.
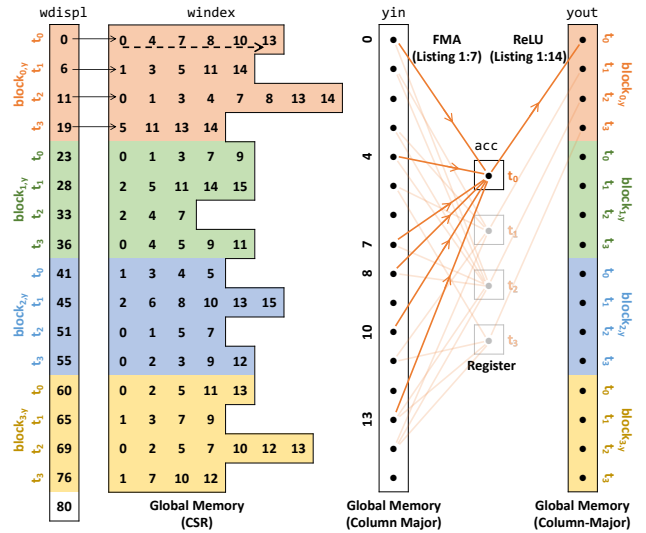

Fig. 1: Baseline fused kernel implementation. Each thread irregularly accesses the input features and accumulates the output in register.

III. PROPOSED ALGORITHM DESIGN

In this section we discuss in detail the three GPU performance optimizations to improve the inference rate of the baseline implementation, and two memory optimizations to fit large models into limited GPU memory. These optimizations involve register tiling, shared memory tiling, efficient access to weight matrix $\boldsymbol{W}_l$, compact index representation and out-of-core storage of weight matrix $\boldsymbol{W}_l$. Listing 2 shows the optimized-fused kernel implementation for sparse DNN computation. Next we will describe each of these optimizations and tuning parameters in detail.

A. GPU Kernel Optimizations

1) Register Tiling: The most obvious inefficiency of the baseline fused kernel (shown in Listing 1, line 11) is the duplicated access to the weight matrix across output features. To provide reuse of the weight matrix $\boldsymbol{W}_l$ from register, the optimized kernel groups (MINIBATCH) multiple active features and performs the ReLU computation for all of them in a single step. This reuses the index (`windex`) and value (`wvalue`) elements in each thread for MINIBATCH features as shown in Listing 2, lines 23 and 24, where MINIBATCH is the number of features in each minibatch.

When MINIBATCH is increased, the register data reuse improves, thus increasing the arithmetic intensity. This saves memory bandwidth for reading the weight matrices, but also increases register useage. A MINIBATCH value of 12 is selected for optimal performance, which balances increased reuse with memory spills from increased register pressure.

2) Shared-Memory Tiling: We now address the duplicate and irregular accesses to input features. Each input feature element is potentially accessed multiple times by multiple threads and they are accessed in an irregular patterns controlled by the weight sparsity pattern expressed by `windex`. This wastes memory bandwidth and increases access latency. For

example, for $block_{0,y}$ in Figure 1, both t_0 and t_2 access yin[4] but at different iterations for their execution.

Listing 2: Optimized Kernel Implementation

```
1   __global__ void opt_ReLU(float *yout, float *yin, int neuron,
2    int *buffdispl, int *mapdispl, unsigned short *map,
3    int *wdispl, unsigned short *windex, float *wvalue,
4    float *bias, int *active, int *category){
5     __shared__ float shared[BUFFSIZE];
6    int wind = threadIdx.x%WARPSIZE;
7    int yoff = blockIdx.y*MINIBATCH;
8    int xoff = blockIdx.x*blockDim.x+threadIdx.x;
9    float acc[MINIBATCH] = {0.0};
10   for(int buff = buffdispl[blockIdx.x];
11       buff < buffdispl[blockIdx.x+1]; buff++){
12     int mapnz = mapdispl[buff+1]-mapdispl[buff];
13     for(int n = threadIdx.x; n < mapnz; n += blockDim.x){
14       int ind = map[mapdispl[buff]+n];
15       for(int f = 0; f < MINIBATCH; f++){
16         shared[f*buffsize+n] = yin[category[yoff+f]*neuron+ind];
17       }
18     __syncthreads();
19     int warp = (buff*blockDim.x+threadIdx.x)/WARPSIZE;
20     for(int m = wdispl[warp]; m < wdispl[warp+1]; m++){
21       int ind = windex[m*WARPSIZE+wind];
22       float val = wvalue[m*WARPSIZE+wind];
23       for(int f = 0; f < MINIBATCH; f++)
24         acc[f] += shared[f*buffsize+ind]*val;
25     }
26     __syncthreads();
27   }
28   for(int f = 0; f < MINIBATCH; f++){
29     acc[f] = __ReLU(acc[f]+bias[xoff]));
30     if(acc[f] > 0){
31       yout[(yoff+f)*neuron+xoff] = acc[f];
32       atomicAdd(active+blockIdx.y*MINIBATCH+f,1);
33     }
34   }
35 }
```

To address this inefficiency, we stage irregular accesses through shared memory. This is supported by preprocessing the windex rows for each thread block and build a preloading list (map) of all the yin elements collectively accessed by all the threads in the thread block. For example, the preload list for $block_{0,y}$ in Figure 1 would be [0,1,3,4,5,7,8,10,11,13,14].

During execution, the thread block will collect these elements into consecutive entries of a buffer array in the shared memory. For example, yin[0] will be loaded into buffer[0], yin[1] into buffer[1], yin[3] into buffer[2], and so on. The required tiling data structures are constructed once prior to inference and are reused from global memory for computation of all features.

The second part of the preprocessing step is to update the windex so that the stored indices become indicies into the buffer. For example, windex for $t_{0,y}$ will be updated from [0, 4, 7, ...] to [0, 3, 5, ...]. During kernel execution, all threads of a thread block cooperatively collect all the needed yin elements into its shared memory.

When input feature access footprint of a thread block is larger than the shared-memory size, the irregular accesses are performed in multiple stagings, as illustrated in Figure 2(a). Assume that the shared memory can only accommodate six yin elements for each thread block, the footprint for $block_{0,y}$ will be divided into two stages. The footprint of each stage is mapped into the buffer array independently. Thus, for $block_{0,y}$, yin[8], yin[10], and yin[13] that are accessed in the second stage are mapped into buffer[0], buffer[1], buffer[3], as illustrated in Figure 2(d).

For each stage, Listing 2, line 12–17, shows loading of feature data to shared memory using the map data structure.
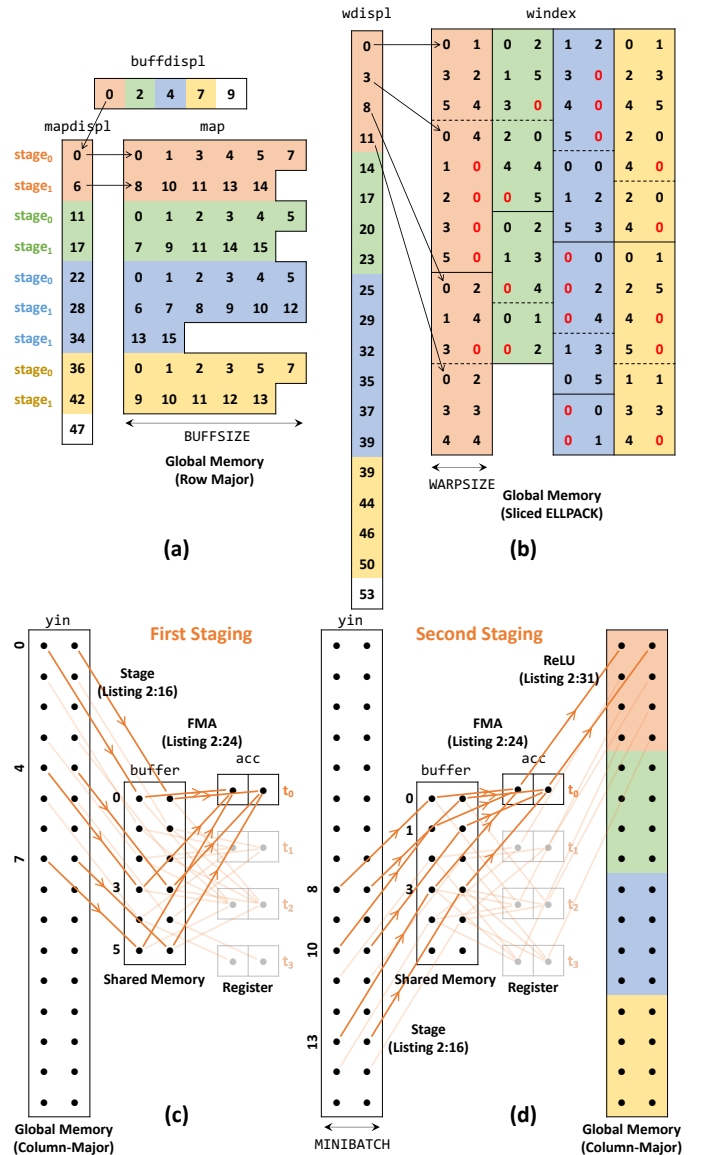

Fig. 2: Optimized-fused kernel execution example.

Then feature data is accessed irregularly from shared memory at line 24 according to the updated address read from windex.

3) Efficient Access to Weight Matrix: Even though the baseline CSR storage is efficient in terms of memory footprint, the access is not coalesced among threads in each warp. To address this, we store the weight matrix in a transposed sliced-ELL storage format with zero-padding in warp granularity. Figure 2 shows the wdispl and windex data structures corresponding to the CSR representation shown in Figure 1.

The first two columns of windex (in orange) in Figure 2(b) shows the layout of the elements for $block_{0,y}$. The top two sections separated by the dashed line each contains the windex elements accessed by a warp of the block during the first stage of execution. The bottom two sections are accessed by the same two warps during their second stage of execution. The wdispl elements marks the positions of the dash lines and solid lines for every warp and every thread block.

The padded zeros are highlighted with red font color. The

TABLE I: Inference Throughput (TeraEdges/Second)

Neurons	Layers	Single V100	Single A100	Number of V100 GPUs (Six per Node)								
				3	6	12	24	48	96	192	384	768
	120	10.51 (0.225s)	16.74 (1.59×)	18.92	22.46	25.52	28.52	27.77	**29.17**	27.89	29.12	29.13
1024	**480**	12.87 (0.073s)	20.99 (1.63×)	21.47	24.34	26.92	28.73	28.43	**29.30**	28.80	29.10	23.06
	1920	14.30 (0.264s)	20.68 (1.45×)	22.26	24.77	27.33	28.70	28.58	28.60	28.73	**28.83**	28.83
	120	9.45 (0.100s)	14.27 (1.51×)	20.69	31.36	47.82	62.03	70.31	75.81	79.11	81.13	**82.20**
4096	**480**	11.74 (0.322s)	18.63 (1.59×)	28.18	40.58	56.54	67.63	73.16	77.27	80.02	79.97	**82.22**
	1920	13.88 (1.08s)	19.86 (1.43×)	30.53	44.48	62.74	72.57	73.72	76.25	79.99	80.67	**82.32**
	120	6.15 (0.614s)	11.60 (1.89×)	16.31	28.85	50.74	64.33	89.18	111.44	**146.88**	114.87	111.30
16384	**480**	7.45 (2.027s)	14.31 (1.92×)	19.82	32.88	50.83	71.45	95.78	112.61	138.62	138.30	**139.44**
	1920	7.84 (7.704s)	15.27 (1.95×)	20.86	33.62	57.08	77.73	104.83	120.63	146.11	146.30	**146.40**
	120	3.47 (4.352s)	8.15 (2.35×)	10.90	18.77	34.20	51.14	73.67	100.72	162.19	173.25	**179.58**
65536	**480**	3.83 (15.769s)	9.08 (2.37×)	12.13	20.39	37.63	56.66	75.29	108.06	166.15	**170.26**	169.30
	1920	3.93 (61.474s)	9.33 (2.37×)	12.47	20.88	38.81	58.08	77.55	112.01	167.43	170.06	**171.37**

dashed lines represents the boundary between warps (each block has two warps in this example) and solid lines represent the boundaries between buffer stages, i.e., all blocks except block 2 involve two stagings and block 3 involves three stagings. In this example, the zero padding overhead is 27.5% for warp granularity, however, it would be 80% and 100% with zero padding in tile and layer granularity, respectively. Warp-level padding introduces a small number of zeros while maintaining coalesced (efficient) memory access.

B. Memory Optimizations

1) Out-of-Core Storage and Overlapping Strategy: Data parallelism provides good scaling in an embarrassingly parallel fashion. However, duplicating weights in each GPU can make large networks infeasible for GPUs with limited memory capacity. As a remedy, we implement an out-of-core storage algorithm that loads the required weight data structures to GPU memory from CPU memory when needed. Even though the out-of-core algorithm saves significant amount of memory, it has a data transfer overhead. We address this overhead by hiding the data transfer behind the GPU kernel with a double-buffering and overlapping strategy.

Double-buffering involves a pair of buffers in the GPU memory. While layer l uses weights from one buffer, weights for layer $l + 1$ are moved into the other buffer. When layer l and the copy are both finished, the buffer pointers are swapped and the same procedure is followed for the next layer. The data transfers are completely hidden behind the inference computation in our implementation.

2) Compact Representation and Batching: In order to reduce the memory footprint, we store the `map` and `windex` data structures with two-byte `unsigned short` data type. That reduces the memory footprint (and hence the data transfer time) by approximately 33%.

We create batches for inputs to further reduce the memory consumed by input and output features during inference computation. Batching has no significant overhead since we overlap transfer of weights during the GPU computation as discussed in § III-B1. As a result, we can fit even the largest inference problem in a single V100 GPU with 16 GB memory.

IV. EVALUATION

A. Experimental Setup

We use the Summit [17] system at Oak Ridge National Laboratory. Summit comprises 4,608 compute nodes, each with six 16 GB V100 GPUs. The network is a non-blocking fat tree of EDR InfiniBand with 23 GB/s node injection bandwidth. The throughput numbers are calculated by calculating input edges over inference time. Inference time includes overlapped data copy time of weight and inputs to the GPUs. Our evaluation is carried out using Spectrum MPI 10.3.1.2, XL compiler 16.1.1, nvcc 10.1.234, and CUDA driver 418.116;

B. Single GPU performance

1) Single Volta V100 GPU performance: The first column of Table I shows the single-GPU throughput of our optimized implementation. Compared to the baseline implementation, our optimizations provide 5.56×–11.84× performance improvement. Thus, we do not report the baseline performance in detail due to lack of space. As the depth of the network increases, the throughput increases due to increased average sparsity in the features. This means more feature rows are entirely zero, and no thread-block is mapped to them. As the number of neurons increases, the throughput decreases due to two effects. First, increased zero-padding in the sliced ELLPACK format causes more wasted work and memory bandwidth. Second, less reuse from shared memory, since a given set of outputs is less likely to reuse the same footprint of features.

2) Single Ampere A100 GPU Performance: We now compare the performance of the optimized fused kernel on the latest GPU, NVIDIA Ampere A100. A100 increases memory capacity from 16 to 40 GB, grows L2 cache from 6MB to

TABLE II: Performance (Edges/Second) and Speedup (×) Comparisons with 2019 Sparse DNN Challenge Submissions

| | | This Work | Bisson & Fatica [18] | | Davis et al. [20] | | Ellis & Rajamanickam [21] | | Wang et al. [22] | | Wang et al. [23] | |
| | | | 2019 Champion | | 2019 Champion | | 2019 Innovation | | 2019 Student Innov. | | 2019 Finalist | |
Neurons	Layers	Throughput	Throughput	Speedup	Throughput	Speedup	Throughput	Speedup	Throughput	Speedup	Throughput	Speedup
1024	120	2.917E+13	4.517E+12	6.46	1.533E+11	190.28	2.760E+11	105.69	1.407E+11	207.32	8.434E+10	345.88
	480	2.930E+13	7.703E+12	3.80	2.935E+11	99.83	2.800E+11	104.64	1.781E+11	164.51	9.643E+10	303.84
	1920	2.883E+13	8.878E+12	3.25	2.754E+11	104.68	2.800E+11	102.96	1.896E+11	152.06	9.600E+10	300.30
4096	120	8.220E+13	6.541E+12	12.57	1.388E+11	592.22	2.120E+11	387.74	1.943E+11	423.06	6.506E+10	1,263.52
	480	8.222E+13	1.231E+13	6.68	1.743E+11	471.72	2.160E+11	380.65	2.141E+11	384.03	6.679E+10	1,230.99
	1920	8.232E+13	1.483E+13	5.55	1.863E+11	441.87	2.160E+11	381.11	2.197E+11	374.69	6.617E+10	1,244.02
16384	120	1.469E+14	1.008E+13	14.57	1.048E+11	1,401.53	1.270E+11	1,156.54	1.966E+11	747.10	3.797E+10	3,867.84
	480	1.394E+14	1.500E+13	9.29	1.156E+11	1,206.23	1.280E+11	1,089.38	2.060E+11	676.89	3.747E+10	3,721.66
	1920	1.464E+14	1.670E+13	8.77	1.203E+11	1,216.96	1.310E+11	1,117.56	1.964E+11	745.52	3.750E+10	3,903.72
65536	120	1.796E+14	9.388E+12	19.13	1.050E+11	1710.29	9.110E+10	1971.24	1.892E11	949.15	–	–
	480	1.703E+14	1.638E+13	10.40	1.091E+11	1,560.59	8.580E+10	1,984.38	1.799E+11	946.41	–	–
	1920	1.714E+14	1.787E+13	9.59	1.127E+11	1,520.59	8.430E+10	2,032.86	–	–	–	–

40MB, and brings 1.73× global memory bandwidth and 1.24× the single-precision floating point peak performance [24]. At the time of writing, the A100 is not available to the public, so we do not have a cluster for scaling studies. We restrict our study to the performance improvement of our optimized-fused kernel on out-of-the box single A100 GPU, without any A100-specific optimizations or tuning. We use CUDA 11 with NVIDIA driver 450.51 on an Ubuntu machine.

Table I shows the performance improvement achieved by the our optimized implementation on Ampere A100 GPU. Using the same code, A100 yields a 1.45× to 2.37× speedup. The improvement is more modest for smaller networks, for which the implementation makes only modest demand on the memory subsystem. For larger networks where the kernel relies more on cache and global memory performance, A100 provides a much larger speedup. Optimization specific to A100's architectural features should yield further improvement.

C. Multi-GPU Scaling on Summit System

In this evaluation, we report scaling of our sparse DNN inference code with the Sparse DNN Challenge dataset. We use MPI to parallelize the inference across multiple GPUs on the Summit system without any network architecture- or topology-specific optimization. This work employs a batch parallelism strategy with an embarrassingly-parallel fashion, where weights are replicated between GPUs and the features are partitioned evenly across GPUs. During the inference, we prune the inactive features, which yields load imbalance between GPUs. Also, when the number of remaining active features per GPU is small, the per-GPU throughput drops significantly. We leave these open problems for future work.

Table I shows the throughput achieved on Summit for all network configurations on up to 768 GPUs. For the smallest network configuration, the strong-scaling limit is 16 nodes (96 GPUs), which is more than the four-GPU scaling limit observed on a *single* node of the 2019 champions. Although strong scaling is observed, the largest parallel efficiency observed is 54% at three nodes. For larger configuration, strong scaling is observed out to 128 nodes (768 GPUs) and corresponds to 223.3 GigaEdges/Second per GPU, and a parallel efficiency of 87.6% is observed for one full node (six GPUs), and 82.6% at two nodes.

D. Comparison with Prior Work

Table II compares the fastest time from our submission with the fastest times from various 2019 submissions. Our speedup varies from 3.25× to 19.13× over the fastest champion from 2019, with one configuration achieving a 1710× speedup over one of the 2019 champions. Part of the contribution is from the kernel implementation: the single-GPU speedup over Bisson & Fatica [18] varies from 4.3× for the 1024-neuron 120-layer to 1.13× for the 65526-neuron 1920-layer configurations.

1) Comparison with cuSPARSE Library: Wang et al. [23] uses cuSPARSE on a V100 in their challenge submission in 2019. Like this work, they do not operate on inactive features, making it possible for a direct comparison. As they report single-GPU inference (the last column of Table II) times on V100, we are able to compare our single-GPU implementation to the fastest results they achieved with cuSPARSE. The speedup of our single-GPU implementation varies from 210× for 4096 neurons / 1920 layers to 125× for 1024 neurons / 120 layers over their cuSPARSE implementation.

V. CONCLUSION

In this work, we discuss that a baseline sparse DNN kernel performance is limited by memory bandwidth and irregular memory accesses. To address this, we propose three performance optimizations: register tiling, shared-memory tiling, and efficient memory access to weight matrices. We scale our implementation up to 768 Volta V100 GPUs and report up to 180 TeraEdges/Second sustained inference throughput. These results are up to 4.3× faster on a single V100 GPU and an order of magnitude faster at scale when compared with 2019 Champions. We also show that proposed implementation when executed with the latest Ampere A100 GPU, without any optimization, achieves up to 2.37× speedup over V100 GPU.

REFERENCES

[1] E. Real, A. Aggarwal, Y. Huang, and Q. V. Le, "Regularized evolution for image classifier architecture search," *Proceedings of the AAAI Conference on Artificial Intelligence*, p. 47804789, Jul 2019.

[2] B. Zoph, G. Ghiasi, T.-Y. Lin, Y. Cui, H. Liu, E. D. Cubuk, and Q. V. Le, "Rethinking pre-training and self-training," *arXiv:2006.06882*, 2020.

[3] M. Shoeybi, M. Patwary, R. Puri, P. LeGresley, J. Casper, and B. Catanzaro, "Megatron-LM: Training multi-billion parameter language models using model parallelism," *arXiv:1909.08053*, 2019.

[4] T. B. Brown, B. Mann, N. Ryder, M. Subbiah, J. Kaplan, P. Dhariwal, A. Neelakantan, P. Shyam, G. Sastry, A. Askell, S. Agarwal, A. Herbert-Voss, G. Krueger, T. Henighan, R. Child, A. Ramesh, D. M. Ziegler, J. Wu, C. Winter, C. Hesse, M. Chen, E. Sigler, M. Litwin, S. Gray, B. Chess, J. Clark, C. Berner, S. McCandlish, A. Radford, I. Sutskever, and D. Amodei, "Language models are few-shot learners," *arXiv:2005.14165*, 2020.

[5] "Exploring massively multilingual, massive neural machine translation https://ai.googleblog.com/2019/10/exploring-massively-multilingual.html," October 2019.

[6] Y. Huang, Y. Cheng, A. Bapna, O. Firat, M. X. Chen, D. Chen, H. Lee, J. Ngiam, Q. V. Le, Y. Wu, and Z. Chen, "GPipe: Efficient training of giant neural networks using pipeline parallelism," *arXiv:1811.06965*, 2018.

[7] S. Han, H. Mao, and W. J. Dally, "Deep compression: Compressing deep neural networks with pruning, trained quantization and Huffman coding," *International Conference on Learning Representations (ICLR)*, 2016.

[8] J. Kepner and R. Robinett, "RadiX-Net: structured sparse matrices for deep neural networks," *2019 IEEE International Parallel and Distributed Processing Symposium Workshops (IPDPSW)*, May 2019.

[9] M. Tan and Q. Le, "EfficientNet: Rethinking model scaling for convolutional neural networks," in *Proceedings of the 36th International Conference on Machine Learning* (K. Chaudhuri and R. Salakhutdinov, eds.), vol. 97 of *Proceedings of Machine Learning Research*, (Long Beach, California, USA), pp. 6105–6114, PMLR, 09–15 Jun 2019.

[10] J. Kepner, S. Alford, V. Gadepally, M. Jones, L. Milechin, A. Reuther, R. Robinett, and S. Samsi, "Graphchallenge.org sparse deep neural network performance," *arXiv:2004.01181*, 2020.

[11] J. Kepner, A. Simon, V. Gadepally, M. Jones, L. Milechin, R. Robinett, and S. Samsi, "Sparse deep neural network graph challenge," *arXiv:1909.05631v1 [cs.CV]*, Sep.2019.

[12] V. S. Mailthody, K. Date, Z. Qureshi, C. Pearson, R. Nagi, J. Xiong, and W.-m. Hwu, "Collaborative (CPU+GPU) algorithms for triangle counting and truss decomposition," in *2018 IEEE High Performance extreme Computing Conference (HPEC'18)*, (Boston, USA), 2018.

[13] C. Pearson, M. Almasri, O. Anjum, V. S. Mailthody, Z. Qureshi, R. Nagi, J. Xiong, and W.-m. Hwu, "Update on triangle counting on GPU," in *2019 IEEE High Performance extreme Computing Conference (HPEC'19)*, (Boston, USA), 2019.

[14] M. Almasri, O. Anjum, C. Pearson, Z. Qureshi, V. S. Mailthody, R. Nagi, J. Xiong, and W.-m. Hwu, "Update on k-truss decomposition on GPU," in *2019 IEEE High Performance extreme Computing Conference (HPEC'19)*, (Boston, USA), 2019.

[15] M. Hidayetoglu, T. Bicer, S. G. de Gonzalo, B. Ren, D. Gursoy, R. Kettimuthu, I. T. Foster, and W.-m. W. Hwu, "MemXCT: Memory-centric X-ray CT reconstruction with massive parallelization," in *International Conference for High Performance Computing, Networking, Storage and Analysis*, (Denver, CO), 2019.

[16] M. Hidayetoglu, T. Bicer, S. G. de Gonzalo, B. Ren, V. De Andrade, D. Gursoy, R. Kettimuthu, I. T. Foster, and W.-m. W. Hwu, "Petascale XCT: 3D image reconstruction with hierarchical communications on multi-GPU nodes," in *International Conference for High Performance Computing, Networking, Storage and Analysis*, (Atlanta, GA), 2020.

[17] "Summit user guide," 2020.

[18] M. Bisson and M. Fatica, "A GPU implementation of the sparse deep neural network graph challenge," in *2019 IEEE High Performance Extreme Computing Conference (HPEC)*, pp. 1–8, IEEE, 2019.

[19] "HPEC Graph Challenge." https://graphchallenge.mit.edu/challenges. Accessed: 2020-01-24.

[20] T. A. Davis, M. Aznaveh, and S. Kolodziej, "Write quick, run fast: Sparse deep neural network in 20 minutes of development time via SuiteSparse: GraphBLAS," in *2019 IEEE High Performance extreme Computing Conference (HPEC)*, pp. 1–6, IEEE, 2019.

[21] J. A. Ellis and S. Rajamanickam, "Scalable inference for sparse deep neural networks using Kokkos kernels," in *2019 IEEE High Performance Extreme Computing Conference (HPEC)*, pp. 1–7, IEEE, 2019.

[22] X. Wang, Z. Lin, C. Yang, and J. D. Owens, "Accelerating DNN inference with GraphBLAS and the GPU," in *2019 IEEE High Performance Extreme Computing Conference (HPEC)*, pp. 1–6, IEEE, 2019.

[23] J. Wang, Z. Huang, L. Kong, J. Xiao, P. Wang, L. Zhang, and C. Li, "Performance of training sparse deep neural networks on GPUs," in *2019 IEEE High Performance Extreme Computing Conference (HPEC)*, pp. 1–5, IEEE, 2019.

[24] "NVIDIA Tesla A100 Tensor Core GPU Architecture." https://www.nvidia.com/content/dam/en-zz/Solutions/Data-Center/nvidia-ampere-architecture-whitepaper.pdf, 2020.